

Scaling law of order- q power spectra for infinite time correlations near band-splitting points

Hiroshi Shibata, Satoshi Ando, and Hirokazu Fujisaka
Department of Physics, Kyushu University 33, Fukuoka 812, Japan
 (Received 20 September 1991)

The description of an infinite number of time correlations associated with band-splitting phenomena in chaotic systems is executed by means of the order- q power spectrum $I_q(\omega)$ which was recently introduced with the aim of elucidating various aspects of time correlations in a dynamical (temporal) fluctuation. By sweeping the value of the parameter q , various parts of dynamical fluctuation are singled out. Just before the band splitting, the temporal evolution of the state variable intermittently switches between two bands. Because of the long-time correlation, the order- q power spectrum exhibits a critical behavior. It will be shown that this is described by the dynamic scaling law $I_q(\omega) = \kappa^{-1} I(q/\kappa, \omega/\gamma_q)$ with $\gamma_q = \kappa \gamma(q/\kappa)$, where κ is a characteristic value of q , which tends to zero as the system approaches the band-splitting point, and γ_q is the width of $I_q(\omega)$. Numerical results are compared with theoretical ones due to a simplified Markovian stochastic model.

PACS number(s): 02.50.+s, 05.45.+b

I. INTRODUCTION

Intermittent switching is a phenomenon in which the phase point stays within a part of an attractor for a time and intermittently migrates into remaining parts of the attractor. Typically it is observed just before the band splitting in chaotic systems. Band splitting is found in various chaotic systems, such as the driven damped pendulum [1,2], the driven Duffing equation [3], the Hénon map, the dissipative standard map [4], and many others.

Recently we have studied the long-time statistical characteristics associated with band splitting with a new approach [5,6]. This approach aims at a statistical description of large fluctuations of a dynamical variable and is especially powerful for intermittent switching as observed in band splitting. Let $P_n(\alpha)$ be the probability density for the finite time-span average with a length n of a dynamical fluctuation representing the band-splitting characteristic to take the value α . $P_n(\alpha)$ takes the asymptotic form $e^{-n\sigma(\alpha)}$ for a large n [7,8]. The fluctuation spectrum $\sigma(\alpha)$ is a fundamental function describing the long-time statistics of the dynamical fluctuation in the sense that it is relevant to how fast fluctuations decay as n goes to infinity. Complementarily introducing the characteristic function $\phi(q)$, q being an intensive variable ($-\infty < q, \infty$), we found the scaling law [9]

$$\phi(q) = \kappa \bar{\phi} \left(\frac{q}{\kappa} \right), \quad \sigma(\alpha) = \kappa \bar{\sigma}(\alpha), \quad (1.1)$$

where κ is the characteristic value of q before the band-splitting point, and evaluate how the control parameter behaves close to the band-splitting point. $\bar{\phi}$ and $\bar{\sigma}$ are scaling functions.

The fluctuation spectrum is unable to single out explicit temporal correlations. As stressed in Ref. [13] by reflecting the spectral structures of finite-span averages, the temporal correlations have infinite aspects. These multicharacteristics are shown to be singled out by the

order- q power spectrum $I_q(\omega)$.

Roughly speaking the order- q power spectrum is a power spectrum calculated with time regions whose average values take the same value $\alpha(q) [= d\phi(q)/dq]$. In this sense it singles out the correlation characteristic specified by the intensive parameter q . The fundamental aim of the present paper is to study the dynamic scaling property of the order- q power spectrum for intermittent switching observed near the band-splitting points of three dynamical systems.

This paper is organized as follows. In Sec. II the theory of the fluctuation spectrum and the order- q power spectrum is briefly reviewed. In Sec. III the dynamic scaling law for the order- q power spectrum is investigated for three chaotic dynamical systems: (i) the logistic parabola, (ii) the double-well potential system subject to periodic external excitation, and (iii) the parametrically excited pendulum. Concluding remarks are given in Sec. IV.

II. INFINITE NUMBER OF TIME CORRELATIONS AND THE ORDER- q POWER SPECTRUM

In the present section we will introduce the order- q power spectrum to single out various correlation characteristics involved in time series. Before going into the discussion of time correlation, let us briefly review the thermodynamic formalism for dynamical (temporal) fluctuations [8,10–12].

Let us take the dynamical fluctuation $\{u_j\}_{j=1}^{nN}$, which is divided into N subregions. The k th subregion has the average value

$$\alpha_n \{k\} = \frac{1}{n} \sum_{j=1}^n u_{j+(k-1)n}. \quad (2.1)$$

The probability density that α_n takes a value α' is represented by

$$P_n(\alpha') \equiv \langle \delta(\alpha_n - \alpha') \rangle \\ = \lim_{N \rightarrow \infty} \frac{1}{N} \sum_{k=1}^N \delta(\alpha_n \{k\} - \alpha'), \quad (2.2)$$

where $\langle \rangle$ is the ensemble average and $P_n(\alpha')$ approaches $\delta(\alpha' - \alpha_\infty)$ as $n \rightarrow \infty$, where α_∞ is the ensemble average of α_n . In many systems $P_n(\alpha')$ asymptotically takes the form [7,8]

$$P_n(\alpha') \sim e^{-n\sigma(\alpha')} \quad (2.3)$$

for large n . The *fluctuation spectrum* $\sigma(\alpha')$ plays an important role for the long-time characterization of $\{u_j\}$.

Let us introduce the characteristic function [8] $\phi(q)$ by

$$M_q(n) \equiv \langle \exp(nq\alpha_n) \rangle = Q_q(n) e^{\phi(q)n}, \quad (2.4)$$

where

$$\phi(q) = \lim_{n \rightarrow \infty} \frac{1}{n} \ln M_q(n). \quad (2.5)$$

The functions $\sigma(\alpha)$ and $\phi(q)$ are related via the Legendre transform

$$\alpha(q) = \frac{d\phi(q)}{dq}, \\ \sigma(\alpha) = q\alpha - \phi(q), \quad (2.6) \\ q = \frac{d\sigma(\alpha)}{d\alpha}.$$

The $\sigma(\alpha)$ function discussed in the present paper and the $f(\alpha)$ of Halsey *et al.* have the same mathematical structure, which is called the thermodynamic formalism. Contrary to the fact that $f(\alpha)$ deals with the distribution of singularities in a strange set, the present $\sigma(\alpha)$ describes the distribution of ‘‘averages’’ over finite time regions in the temporal fluctuation. The above thermodynamic functions cannot describe the explicit time correlations embedded in $\{u_j\}$ because, as seen in (2.1), $\alpha_n \{k\}$ is invariant under any change of $u_{(k-1)n}, u_{(k-1)n+1}, u_{(k-1)n+2}, \dots, u_{(k-1)n+n}$. One easily sees that the explicit temporal correlations are contained in $Q_q(n)$. However in order to ascertain the explicit time correlations it is convenient to use the *order- q power spectrum* $I_q(\omega)$ defined as [13]

$$I_q(\omega) \equiv \lim_{n \rightarrow \infty} \langle F_n(\omega) \delta(\alpha_n - \alpha(q)) \rangle / P_n(\alpha(q)), \quad (2.7)$$

where

$$F_n(\omega) \equiv \left| \frac{1}{\sqrt{n}} \sum_{j=0}^{n-1} u_j e^{-i\omega j} \right|^2 \quad (2.8)$$

is the spectral intensity. $I_q(\omega)$ is the power spectrum over time regions where the averages α_n take the same value $\alpha(q)$. From many subregions we take subregions

$$v_{\pm}(q) = \frac{h'_{12}e^q + h'_{21}e^{-q} \pm (\{h'_{12}e^q - h'_{21}e^{-q}\}^2 + 4h'_{12}h'_{21})^{1/2}}{2}. \quad (3.3)$$

Its largest eigenvalue determines the characteristic function $\phi(q)$ as

whose averages are all $\alpha(q)$ and calculate the power spectrum with them. This is hereafter called the microcanonical method. There is another way to get $I_q(\omega)$ [13]. By noting the asymptotic behaviors $P_n(\alpha) \sim e^{-n\sigma(\alpha)}$ and $M_q(n) \sim e^{\phi(q)n}$, the order- q power spectrum (2.7) can be rewritten as

$$I_q(\omega) = \lim_{n \rightarrow \infty} \langle F_n(\omega) e^{qn\alpha} \rangle / M_q(n). \quad (2.9)$$

We call this the canonical method. In some cases this expression is more convenient than the formula (2.7).

In general, if there is no continuous branch of eigenvalues, $I_q(\omega)$ is obtained as [13],

$$I_q(\omega) = \frac{1}{2} \sum_l' \frac{K_q^{(l)} \sinh[\gamma_q^{(l)} + i\omega_q^{(l)}]}{\sinh^2 \left[\frac{\gamma_q^{(l)} + i\omega_q^{(l)}}{2} \right] + \sin^2 \left[\frac{\omega}{2} \right]} \quad (l \neq 0). \quad (2.10)$$

Here the $K_q^{(l)}$'s are expansion coefficients (see the Appendix), and \sum_l' means summation over l except $l=0$ corresponding to the largest eigenvalue. $\gamma_q^{(l)}$ is a decay rate and $\omega_q^{(l)}$ is a characteristic frequency in subtime series specified by the parameter value q .

Furthermore $Q_q(n)$ is usually written as [14]

$$Q_q(n) = J_q^{(0)} + \sum_{l'} J_q^{(l)} e^{-(\gamma_q^{(l)} + i\omega_q^{(l)})n}. \quad (2.11)$$

Therefore the poles of the order- q power spectrum agree with the complex decay rates in $Q_q(n)$.

III. DYNAMIC SCALING LAWS FOR BAND MERGING

Before going into concrete calculations, let us briefly discuss the generalized transition-matrix approach [14–16] in the two-state Markov model which plays a significant role near the band-merging point. Let α_i , ($i=1,2$) be a typical value in the i th state. Let $p_i(j)$ be the probability that the phase point at time j is in the i th state ($p_1 + p_2 = 1$). The Markov process can be written as

$$p(j+1) = Hp(j), \quad (3.1)$$

where $p(j) = \text{col}(p_1(j), p_2(j))$. $H = \{H_{ij}\}$ is the transition matrix ($\sum_{i=1}^2 H_{il} = 1$), which yields the steady-state distribution $p_* (= Hp_*)$. So we consider the following generalized transition matrix:

$$H_q = \begin{pmatrix} h'_{21}e^{-q} & h_{12}e^q \\ h_{21}e^{-q} & h'_{12}e^q \end{pmatrix} \quad (h'_{ij} \equiv 1 - h_{ij}), \quad (3.2)$$

where we set $\alpha_1 = -1$ and $\alpha_2 = 1$ without loss of generality. The eigenvalues v_q of H_q give $\phi(q)$, γ_q , $I_q(\omega)$, etc. (see the Appendix). The eigenvalues of H_q are

$$\phi(q) = \ln \frac{h'_{12}e^q + h'_{21}e^{-q} + ((h'_{12}e^q - h'_{21}e^{-q})^2 + 4h_{12}h_{21})^{1/2}}{2}, \tag{3.4}$$

which yields

$$\alpha(q) = \frac{h'_{12}e^q - h'_{21}e^{-q}}{[(h'_{12}e^q - h'_{21}e^{-q})^2 + 4h_{12}h_{21}]^{1/2}}. \tag{3.5}$$

By putting $h'_{21}e^{-q} - h'_{12}e^q = A$ Eq. (3.5) is solved as

$$A = -\frac{\sqrt{4h_{12}h_{21}}}{\sqrt{1-\alpha^2}} \alpha. \tag{3.6}$$

So we get

$$\sigma(\alpha) = -\alpha \ln \frac{A + (A^2 + 4h'_{12}h'_{21})^{1/2}}{2h'_{21}} - \ln \frac{(A^2 + 4h'_{12}h'_{21})^{1/2} + (A^2 + 4h_{12}h_{21})^{1/2}}{2}. \tag{3.7}$$

The order- q power spectrum is obtained, provided that $h_{12} + h_{21} < 1$, as

$$I_q(\omega) = \frac{K_q \sinh(\gamma_q)}{2 \left[\sinh^2 \left[\frac{\gamma_q}{2} \right] + \sin^2 \left[\frac{\omega}{2} \right] \right]}, \tag{3.8}$$

where

$$\gamma_q = \ln \left[\frac{h'_{12}e^q + h'_{21}e^{-q} + [(h'_{12}e^q - h'_{21}e^{-q})^2 + 4h_{12}h_{21}]^{1/2}}{h'_{12}e^q + h'_{21}e^{-q} - [(h'_{12}e^q - h'_{21}e^{-q})^2 + 4h_{12}h_{21}]^{1/2}} \right] \tag{3.9}$$

and

$$K_q = \frac{4h_{12}h_{21}}{(h'_{12}e^q - h'_{21}e^{-q})^2 + 4h_{12}h_{21}}. \tag{3.10}$$

We set $h_{21} = \kappa$, $h_{12} = b\kappa$, and take the limit $\kappa \rightarrow 0$, which means that the two states are two parts of an attractor, respectively. In the limit $q \rightarrow 0$, $\kappa \rightarrow 0$ by keeping $x = q/\kappa$ finite, the following scaling laws hold:

$$\sigma(\alpha) = \kappa \bar{\sigma}(\alpha), \tag{3.11}$$

$$\bar{\sigma}(x) = \frac{1+b}{2} + \frac{b-1}{2}x - [b(1-x^2)]^{1/2}, \tag{3.12}$$

$$I_q(\omega) = \frac{1}{\kappa} I \left[\frac{q}{\kappa}, \frac{\omega}{\gamma_q} \right], \quad \gamma_q = \kappa g \left[\frac{q}{\kappa} \right], \tag{3.13}$$

where the scaling functions are

$$I(x, y) = \frac{b}{\left[x^2 - x(b-1) + \left[\frac{b+1}{2} \right]^2 \right]^{3/2}} \frac{1}{1+y^2}. \tag{3.14}$$

$$g(x) = [4x^2 - 4(b-1)x + (b+1)^2]^{1/2}. \tag{3.15}$$

If we set $b = 1$ the two attracting states are statistically equivalent, and the scaling functions are written as $\bar{\sigma}(x) = 1 - (1-x^2)^{1/2}$ and $I(x, y) = (x^2 + 1)^{-3/2} (1 + y^2)^{-1}$. This situation holds for the following three different concrete examples.

A. Logistic parabola

We take the logistic map

$$X_{t+1} = F(X_t) = a - X_t^2. \tag{3.16}$$

As the control parameter a is increased, two chaotic bands merge into one band at $a = a_1 \approx 1.543\,689$ [6,17]. The attractor consists of two bands for just below $a = a_1$ as shown in Fig. 1. At $a = a_1$ the two bands collide with an unstable fixed point and continuously merge into one band for $a > a_1$. An orbit $\{X_{2t}\}$ ($t=0, 1, 2, \dots$) of the secondly iterated map $F \circ F(X)$ stays within one of the two bands for a long mean lifetime τ and then intermittently hops into the other. Let us set

$$u = \begin{cases} +1, & X_{2t} > X_* \\ -1, & X_{2t} < X_* \end{cases}, \tag{3.17}$$

where X_* means the fixed point of $F \circ F(X)$.

Figure 2(a) shows how the order- q power spectrum $I_q(\omega)$ changes for different values of q ($=0.0, 0.005, 0.01, 0.015$), for $\epsilon \equiv (a - a_1)/a_1 = 0.000\,17$ being fixed. We used the canonical method by putting $n = 2^{10}$, and the number of each ensemble is 2×10^4 . The comparison of the scaling form with the theoretical result (3.8) is shown in Fig. 2(b). The solid line is the Lorentzian, where the decay rate γ_q was obtained from the half

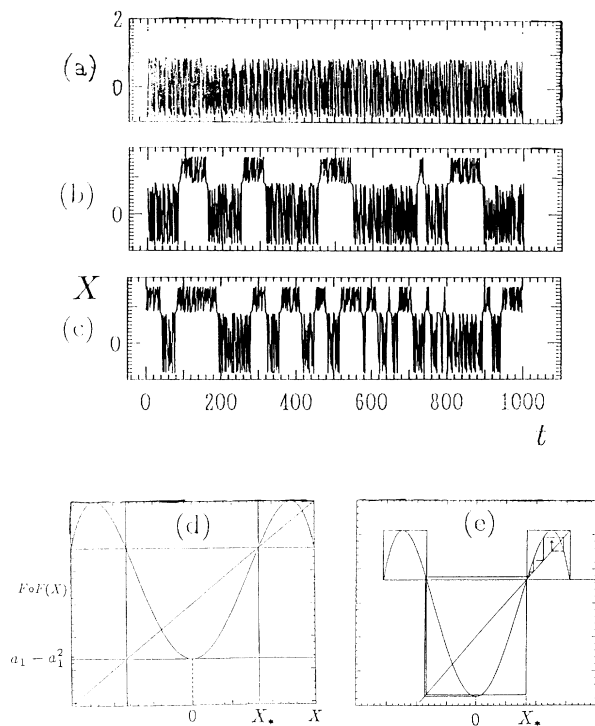


FIG. 1. Time series $\{X_{2t}\}$ ($t=0,1,2,\dots$) of logistic parabola before band merging (a) and after band merging (b) and (c), where the ϵ 's are -5.77×10^{-5} , 7.19×10^{-5} , and 2.66×10^{-4} , respectively. (d) and (e) are $F \circ F(X)$, respectively, for $\epsilon=0$ and a small ϵ ($0 < \epsilon \ll 1$).

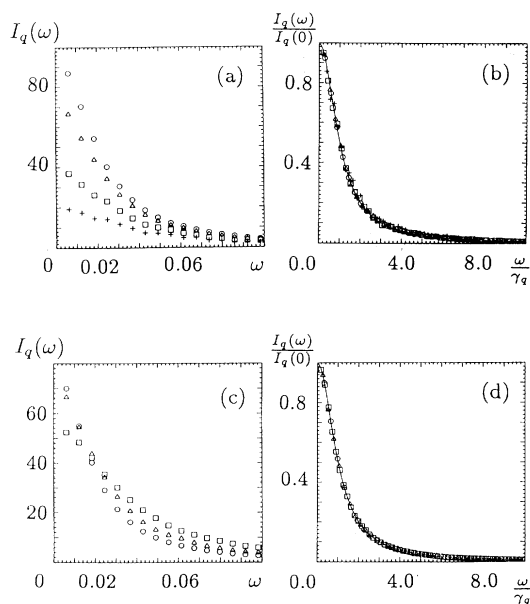


FIG. 2. Order- q power spectra $I_q(\omega)$ for the time series of the coarse-grained position u for the logistic parabola. In (a) ϵ is set to be 0.00017 and $q=0.0$ (\circ), 0.005 (\triangle), 0.01 (\square), 0.015 ($+$). (b) is the scaled form. In (c) q is set to be 0.005 and $\epsilon=0.0001$ (\circ), 0.00017 (\triangle), 0.0004 (\square). (d) is the scaled form of (c). The solid lines are the Lorentzian. For details, see the text.

width of $I_q(\omega)$.

Numerical results of order- q power spectra for $\epsilon=(\frac{1}{100})^2$, $(\frac{1}{75})^2$, and $(\frac{1}{50})^2$ for a fixed q value ($=0.005$) are shown in Fig. 2(c). From this we find that the scaling law of $I_q(\omega)$ holds. The line shape is well explained by the single Lorentzian. The decay rates γ_q are calculated from the half widths of $I_q(\omega)$ which are shown in Fig. 3. The solid line is the theoretical scaling form $g(x)=2(1+x^2)^{1/2}$. We conclude that the order- q power spectrum satisfies the (dynamic) scaling law and the scaling functions are well approximated by those derived from the simplified two-state Markov model.

B. Double-well potential system subject to periodic external excitation

The particle motion in the potential $U(x)$ subject to periodic external excitation obeys

$$\ddot{x}(t) = -\gamma\dot{x} - \frac{dU(x)}{dx} + F \cos(\omega_e t), \quad (3.18)$$

where $x(t)$ is the particle position at time t and γ is the damping rate. F and ω_e are the amplitude and the angular frequency of the external excitation, respectively. The $U(x)$ is the double-well potential,

$$U(x) = \frac{1}{2}c_1x^2 + \frac{1}{4}c_2x^4, \quad (3.19)$$

where $c_1(<0)$ and $c_2(>0)$ are constants, and $U(-x)=U(x)$ and $U(x)$ has two minima at $x_{\pm} = \pm\sqrt{-c_1/c_2}$. In the present paper F is chosen as the control parameter and other parameter values are set as $c_1 = -10$, $c_2 = 100$, $\gamma = 1$, and $\omega_e = 3.5$ [5,18,19].

As was already reported in Ref. [18], for $F < F_*$ ≈ 0.84925 the particle stays within one valley. From the space-inversion symmetry, which valley it remains is uniquely determined by the initial condition. Above F_* the particle migrates between two valleys and intermittently hops from one to the other. As F departs from F_* the mean duration τ in one valley decreases. In order to see the long-time statistics of position fluctuations we observe the particle position at times $t_n = 2\pi n / \omega_e$ ($n=0,1,2,\dots$). Figures 4(a)–4(c) show the temporal evolutions of the particle position. Figures 4(d) and 4(e) display the change of the phase portrait near

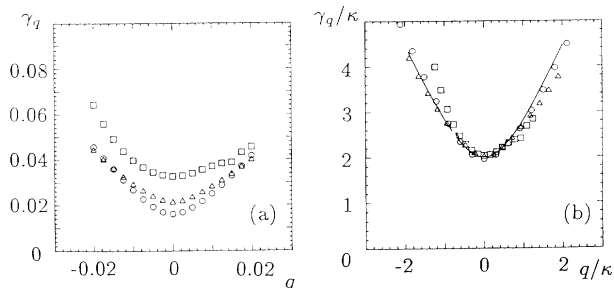


FIG. 3. (a) The half-width γ_q of $I_q(\omega)$ for $\epsilon=0.0001$ (\circ), 0.00017 (\triangle), and 0.0004 (\square). Figure (b) is the γ_q/κ vs q/κ plot of data(a). The symbols are the same as in (a). The solid line is $\gamma_q/\kappa=2[(q/\kappa)^2+1]^{1/2}$.

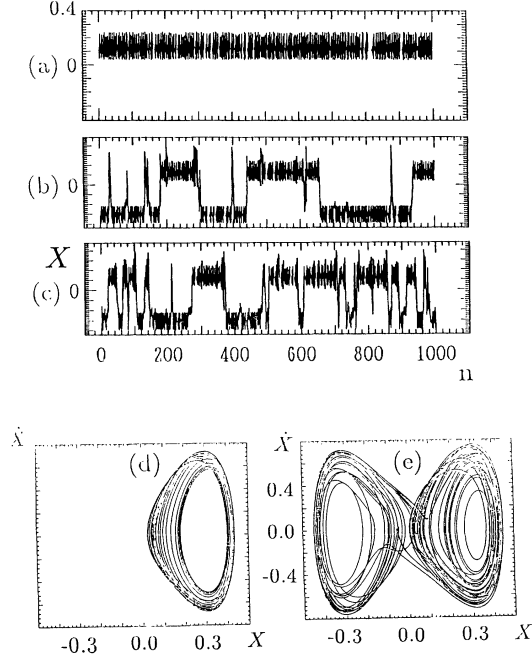


FIG. 4. Typical time series before band merging (a) and after merging (b) and (c). The ϵ values are (a) 2.94×10^{-4} (b) 2.65×10^{-3} , and (c) 7.36×10^{-3} , respectively. Slightly after the band merging the intermittent hopping is clearly observed. The phase portraits are shown before band merging for $F=0.8$ (d) and after band merging for $F=0.865$ (e).

$F = F_*$. Let us take

$$u_n = +1, \quad x(t_n) > 0 \quad (3.20)$$

$$u_n = -1, \quad x(t_n) < 0.$$

The order- q power spectra are calculated for $q=0.0, 0.005, 0.01,$ and 0.015 [Fig. 5(a)], for $\epsilon \equiv (F - F_*)/F_* = 2.24 \times 10^{-3}$. Scaling for the order- q power spectrum is shown in Fig. 5(b), where γ_q was obtained by the half width of $I_q(\omega)$. Figure 5(c) shows the results for $q=0.005$ and for different values of ϵ , $\epsilon = 2.65 \times 10^{-3}, 2.24 \times 10^{-3},$ and 1.47×10^{-3} . We take $n=2^9$ and the number of the ensemble is set as 20×60 . Figure 5(d) is its scaling relation. Furthermore Fig. 6 shows numerical results of the decay rates γ_q derived for the logistic parabola. γ_q turns out to satisfy the dynamic scaling law for $\kappa = 8.17 \times 10^{-3}, 1.10 \times 10^{-3},$ and 1.61×10^{-2} as shown in Fig. 6.

C. Parametrically excited pendulum

As the third example let us take a system obeying the equation of motion

$$\ddot{x} = -k\dot{x} - [a + A \cos(\omega_e t)] \sin 2\pi x, \quad (3.21)$$

where k is a damping rate, $\sqrt{2\pi a}$ is the proper frequency of damped oscillation without excitation, A is the strength of the periodic external force, and ω_e is the frequency of

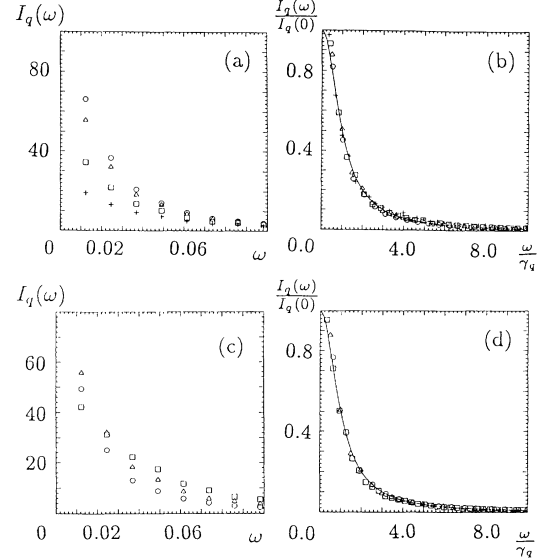


FIG. 5. The order- q power spectra of the coarse-grained particle position for double-well potential system. In (a) and (b) $\epsilon = 2.24 \times 10^{-3}$ and $q = 0.0$ (\circ), 0.005 (\triangle), 0.01 (\square), 0.015 ($+$). In (c) and (d) q is set to be 0.005 and $\epsilon = 1.47 \times 10^{-3}$ (\circ), 2.24×10^{-3} (\triangle), 2.65×10^{-3} (\square). γ_q are the half widths of $I_q(\omega)$. The solid lines in (b) and (d) are the theoretical results based on the simplified two-state stochastic model. Figures (b) and (d) imply the dynamic scaling law.

external force. This equation describes, for example, a pendulum excited by periodically changing the length of the pendulum and also the particle motion in the periodic potential whose amplitude is externally modulated. This system has a space-inversion symmetry ($x \rightarrow -x$). A is hereafter chosen as a control parameter, by setting $k=0.2, a=1/2\pi,$ and $\omega_e=2.0$ [20].

By controlling the value of A , this system shows various phases of motion. At $A=0$ the motionless state $(x, \dot{x}) = (0, 0)$ is stable. As A increases, this fixed point becomes unstable at a certain critical amplitude A_c , and a limit cycle is generated. As A is further increased, the system begins to exhibit the diffusive motion in x space for a certain region of A . This motion was reported previously [21]. To evaluate the long-time diffusive charac-

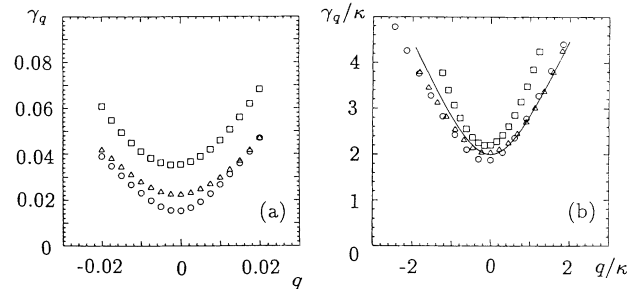


FIG. 6. (a) The damping constant γ_q obtained from $I_q(\omega)$ for $\epsilon = 1.47 \times 10^{-3}$ (\circ), 2.24×10^{-3} (\triangle), and 2.65×10^{-3} (\square). In (b) γ_q/κ vs q/κ are plotted by use of data in (a). The symbols are the same as in (a). The solid line is the same as in Fig. 3.

teristics we introduce quantities obtained by the stroboscopic plot as follows:

$$x_n \equiv x(nT_0), \quad \dot{x}_n \equiv \dot{x}(nT_0), \quad (3.22)$$

$$N_n \equiv [x_n], \quad (3.23)$$

$$u_n \equiv N_{n+1} - N_n, \quad (3.24)$$

where $T_0 (\equiv 2\pi/\omega_e)$ is the period of the external force and $[]$ is Gauss's notation. N_n stands for the valley number where the particle stays at the time step n , and u_n is the coarse-grained jumping number since the time step n to $n+1$.

When A is slightly below $A^* = 0.3326\dots$, u_n takes either $+1$ or -1 depending on the initial condition. This corresponds to a drift motion (rotation) on either the right or left side on the average [Fig. 7(a)]. A stroboscopic plot shows that two statistically equivalent attractors exist, which correspond to the drift motion on the right or left side (Fig. 8), and these are not connected with each other. Above A^* , u_n can take three values $1, 0$, and -1

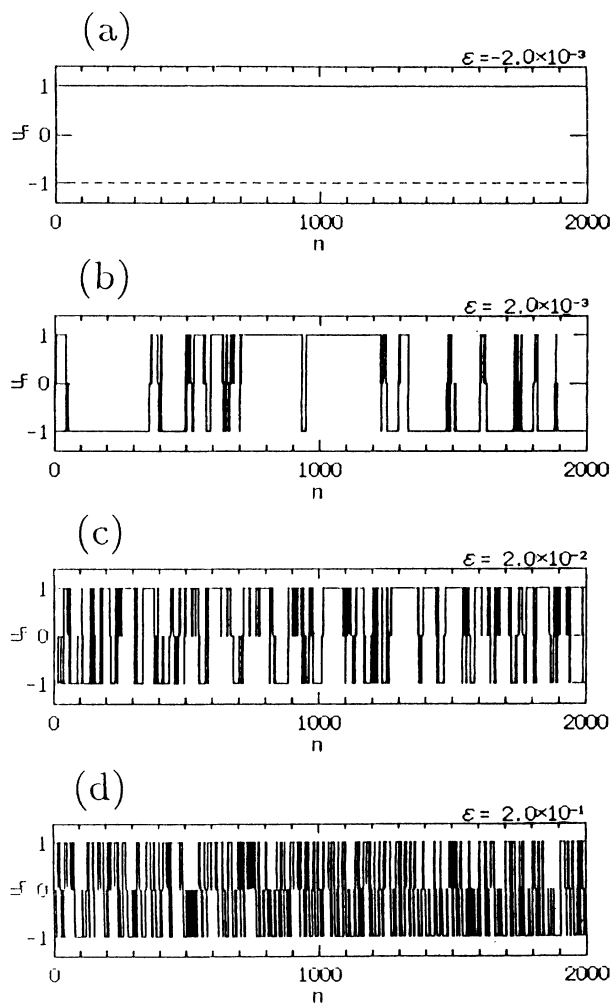


FIG. 7. Typical temporal evolution of rotating rate in a parametrically excited pendulum before band merging (a) and after band merging (b), (c), and (d).

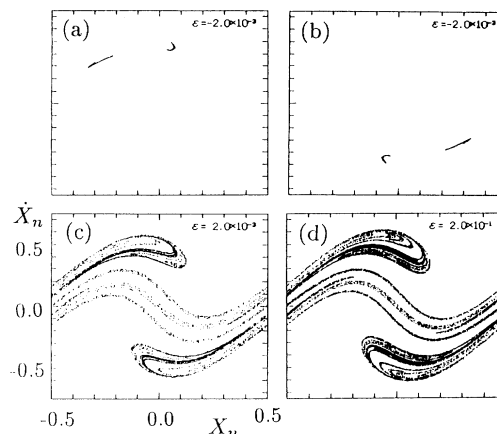


FIG. 8. Stroboscopic plot (x_n, \dot{x}_n) before and after band merging. This shows that there exist two equivalent attractors for $\epsilon < 0$, depending on the initial condition (a) and (b), and one attractor for $\epsilon > 0$, independently of the initial condition (c) and (d).

for almost any initial condition, and intermittently hops from one value to another except the transition from 1 to -1 and vice versa. In this sense for $A > A^*$ there is one attractor. The Poincaré section shows two parts of an attractor and one repeller coexist, and the system exhibits the intermittent switching from one attracting set to the other through the repeller as shown in Figs. 7 and 8. We hereafter study this intermittent switching of time series $\{u_n\}$ ($n=0, 1, 2, \dots$) by means of the fluctuation spectrum and the order- q power spectrum.

At first the thermodynamic quantities $\phi(q)$, $\alpha(q)$, $\chi(q) [\equiv d\alpha(q)/dq]$, and $\sigma(\alpha)$ are calculated with the two-pole approximation, which is shown in Fig. 9 for several values of $\epsilon [\equiv (A - A^*)/A^*]$. The static scaling laws

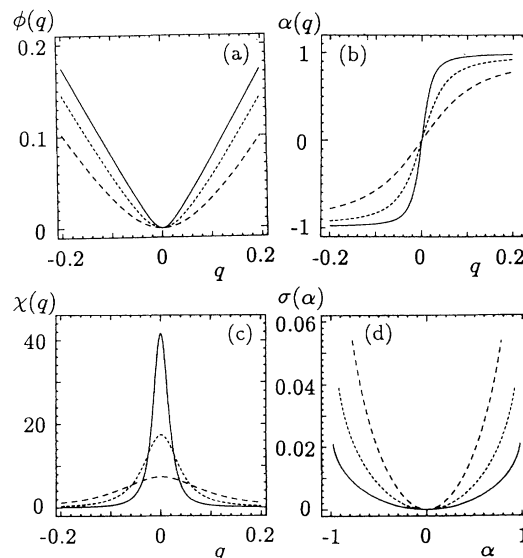


FIG. 9. Characteristic functions obtained with the two-pole approximation. ϕ vs q (a), α vs q (b), χ vs q (c), and σ vs α (d) are calculated, respectively, for $\epsilon = 2.0 \times 10^{-3}$ (—), 2.0×10^{-2} (⋯), and 2.0×10^{-1} (---). As $\epsilon \rightarrow 0$ the thermodynamic functions exhibit critical behaviors.

$$\phi(q) = \kappa \bar{\phi}(q/\kappa), \quad \alpha(q) = \bar{\alpha}(q/\kappa), \quad (3.25)$$

$$\chi(q) = \frac{1}{\kappa} \bar{\chi}(q/\kappa), \quad \sigma(\alpha) = \kappa \bar{\sigma}(\alpha) \quad (3.26)$$

hold as shown in Fig. 10. The solid lines are the results from the two-state model by setting $b=1$. In the level of time series $\{u_n\}$ the expanded time series resemble the time series whose transition probability is small.

Dynamic properties are studied with power spectra. The κ 's were numerically obtained by the slopes of $\alpha(q)$ obtained with $\phi(q)$ which was numerically calculated according to the original definition $\phi(q) \equiv n^{-1} \ln M_q(n)$ with a sufficiently large averaging span n . For $\epsilon = 1.0 \times 10^{-2}$, 8.0×10^{-3} , and 2.0×10^{-3} , the κ values are found, respectively, to be 1.44×10^{-2} , 1.09×10^{-2} , and 6.97×10^{-3} . Figure 11(a) shows how $I_q(\omega)$ changes for different values of q ($=0.0, 0.005, 0.01, 0.015$) for $\epsilon = 8.0 \times 10^{-3}$ being fixed, where the span length is chosen as $n=2^9$, and the number of each ensemble is 20×60 . The canonical method is used for the calculation of $I_q(\omega)$. $I_q(\omega)/I_q(0)$ are plotted in Fig. 11(b) with the use of data in Fig. 11(a). The damping rates γ_q were evaluated from the half widths of $I_q(\omega)$. The solid line in Fig. 11(b) is the theoretical result, the Lorentzian. Numerical results for $\epsilon = 2.0 \times 10^{-3}$, 8.0×10^{-3} , and 2.0×10^{-2} for $q=0.005$ are shown in Fig. 11(c). From this $I_q(\omega)$ turns out to be scaled as the Lorentzian. γ_q 's evaluated from $I_q(\omega)$ are given in Fig. 12. The solid line is $g(x) = 2(1+x^2)^{1/2}$ which is from the two-state model. As the system approaches the transition point the effect of the repeller decreases. This is seen in Fig. 12(b) for $\kappa = 1.44 \times 10^{-2}$, 1.09×10^{-2} , and 6.97×10^{-3} . So, as the system approaches the transition point the γ_q 's become well approximated by the theoretical result due to the simplified two-state model.

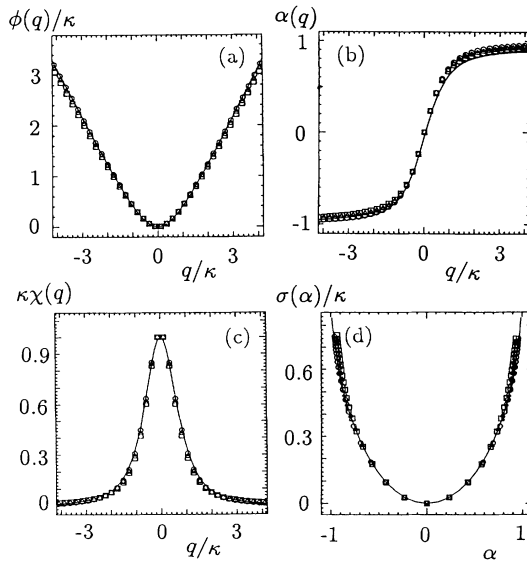


FIG. 10. Scaled thermodynamic functions are plotted for $\epsilon = 2.0 \times 10^{-3}$ (\circ), 2.0×10^{-2} (Δ), and 2.0×10^{-1} (\square). The solid lines are the theoretical curves for $b=1$ in the simplified two-state model. The thermodynamic functions satisfy the static scaling law.

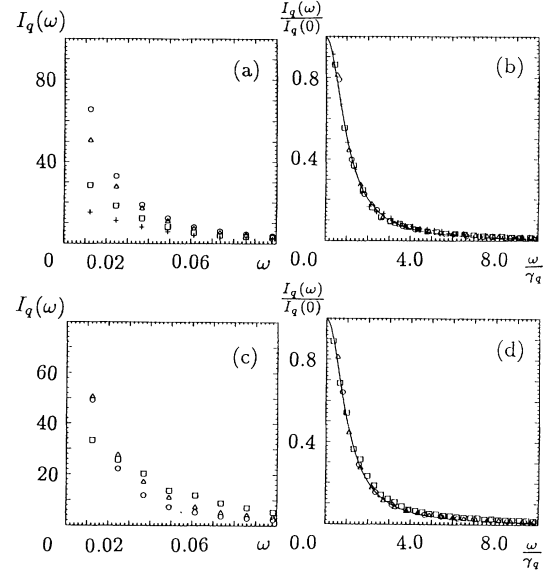


FIG. 11. The order- q power spectra for the rotating rate of the parametrically excited pendulum. In (a) and (b) $\epsilon = 2.0 \times 10^{-2}$ and $q = 0.0$ (\circ), 0.005 (Δ), 0.01 (\square), 0.015 ($+$). In (c) and (d) $q = 0.005$ and $\epsilon = 2.0 \times 10^{-3}$ (\circ), 8.0×10^{-3} (Δ), 2.0×10^{-2} (\square). The solid lines are the same as in Fig. 2. The dynamic scaling law holds for the order- q power spectrum.

IV. CONCLUDING REMARKS

It was shown that the order- q power spectrum satisfies the dynamic scaling law just before the band-splitting point.

By keeping the control parameter fixed, the order- q power spectrum has a Lorentzian shape, which implies that the time correlation decays exponentially. We also calculated the decay rate γ_q of the order- q time correlation, which is the Fourier transform of the order- q power spectrum. Just before the band-splitting point, for the three systems investigated the γ_q are concave with respect to q , and tend to vanish for $q=0$ as the systems approach the transition points (critical slowing down). Near the band-splitting point, the order- q power spectrum $I_q(\omega)$ and the linewidth (decay rate) γ_q turn out to obey the dynamic scaling law with the scaling function

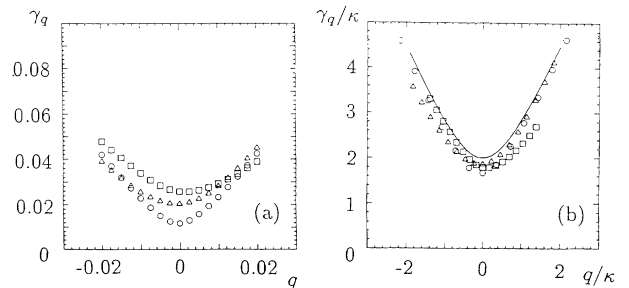


FIG. 12. (a) The damping rate γ_q obtained from $I_q(\omega)$ for $\epsilon = 2.0 \times 10^{-3}$ (\circ), 8.0×10^{-3} (Δ), and 1.0×10^{-2} (\square) in (a). In (b) γ_q/κ vs q/κ are plotted by use of data in (a). The symbols are the same as in (a). The solid line is the same as in Fig. 3.

(3.15) derived from the simplified two-state Markov model.

Present analyses are based on the fact that two or three eigenvalues become degenerate near the band-splitting point. Recently Just and one of the present authors obtained general expressions for the thermodynamic functions and for the linewidth when two or three eigenvalues of the generalized transition matrix become degenerate at certain control parameter values [22]. The present results agree with their general results. However when many poles are degenerate the two-pole approximation or the three-pole approximation of the characteristic function $M_q(n)$ cannot be used, and the order- q power spectrum is not a superposition of Lorentzians.

In the present paper we showed that a dynamical fluctuation has an infinite number of temporal correlations. We again stress that almost all of them cannot be explained with the ordinary power spectrum, which is relevant only to the $q=0$ statistical characteristic of the dynamical function.

APPENDIX: ORDER- q POWER SPECTRUM FOR THE FINITE-STATE MARKOV MODEL

We derive the order- q power spectrum for the Markovian stochastic process. The probability of the i th state at the n th time step is presented by $p_i(n)$ [$\sum_i p_i(n)=1$]. The probability $p(n)$ at the n th step

$$p(n) = \text{col}(p_1(n), p_2(n), \dots, p_m(n)) \quad (\text{A1})$$

obeys the evolution equation

$$p(n+1) = Hp(n), \quad (\text{A2})$$

where H is the transition matrix with the $\mu\nu$ element $H_{\mu\nu}$. The normalization condition requires

$$\sum_{\mu} H_{\mu\nu} = 1. \quad (\text{A3})$$

The invariant probability is the solution of

$$p_{\star} = Hp_{\star}. \quad (\text{A4})$$

Let u_j take the value $v^{(\mu)}$ if u_j is in the μ th state ($\mu=1, 2, \dots, m$). Its average over n time steps is given by

$$\alpha_n = \frac{1}{n} \sum_{j=0}^{n-1} u_j. \quad (\text{A5})$$

In order to evaluate the order- q power spectrum for the m -state Markov model, we use the definition (2.9). Let us introduce the generalized transition matrix H_q with the $\mu\nu$ element

$$(H_q)_{\mu\nu} \equiv H_{\mu\nu} \exp[qv^{(\nu)}]. \quad (\text{A6})$$

Its eigenvalue equation is written as

$$H_q |q, l\rangle = v_q^{(l)} |q, l\rangle, \quad (\text{A7})$$

where $|q, l\rangle$ is the eigenvector corresponding to the eigenvalue $v_q^{(l)}$. We set

$$v_q^{(0)} \equiv \max_l \{ |v_q^{(l)}| \}, \quad (\text{A8a})$$

$$\frac{v_q^{(l)}}{v_q^{(0)}} = e^{-(\gamma_q^{(l)} + i\omega_q^{(l)})}. \quad (\text{A8b})$$

By defining

$$(v)_{\mu\nu} \equiv v^{(\mu)} \delta_{\mu\nu},$$

the matrix v is assumed to be uniquely expanded as

$$v |q, l\rangle = \sum_{l'} a_q(l, l') |q, l'\rangle, \quad (\text{A9})$$

where $a_q(l, l')$ is obtained as follows. Using the adjoint vector $\langle q, l''|$, we get

$$\langle q, l''|v |q, l\rangle = \sum_{l'} \langle q, l''|q, l'\rangle a_q(l, l'). \quad (\text{A10})$$

By introducing the matrices v_q and k_q with the elements

$$(v_q)_{l'l} \equiv \langle q, l''|v |q, l\rangle, \quad (k_q)_{l'l} \equiv \langle q, l''|q, l'\rangle, \quad (\text{A11})$$

Eq. (A11) can be easily solved to yield

$$a_q(l, l') = [k_q^{-1} v_q]_{l'l}, \quad (\text{A12})$$

k_q^{-1} being the inverse matrix of k_q .

After a tedious calculation using those equations we finally arrive at the formula (2.10) with the expansion coefficients [13]

$$K_q^{(l)} = a_q(0, l) a_q(l, 0) \quad (l \neq 0). \quad (\text{A13})$$

[1] E. G. Gwinn and R. M. Westervelt, *Phys. Rev. A* **33**, 4143 (1986).
 [2] D. D'Humieres, M. R. Beasley, B. A. Huberman, and A. Libchaber, *Phys. Rev. A* **26**, 3483 (1982).
 [3] K. Tomita, H. Hata, T. Horita, H. Mori, T. Morita, H. Okamoto, and H. Tominaga, *Prog. Theor. Phys.* **81**, 1124 (1989).
 [4] K. Tomita, H. Hata, T. Horita, H. Mori, and T. Morita, *Prog. Theor. Phys.* **80**, 953 (1988).
 [5] H. Ishii, H. Fujisaka, and M. Inoue, *Phys. Lett. A* **116**, 257 (1986).
 [6] H. Shibata, S. Kuroki, and H. Mori, *Prog. Theor. Phys.* **83**, 829 (1990).

[7] R. S. Ellis, *Entropy, Large Deviations and Statistical Mechanics* (Springer-Verlag, New York, 1985).
 [8] H. Fujisaka and M. Inoue, *Prog. Theor. Phys.* **77**, 1334 (1987).
 [9] H. Fujisaka, A. Yamaguchi, and M. Inoue, *Prog. Theor. Phys.* **81**, 1146 (1989).
 [10] D. Ruelle, *Thermodynamic Formalism* (Addison-Wesley, Reading, MA, 1978).
 [11] H. Fujisaka, *Prog. Theor. Phys.* **70**, 1264 (1983); **71**, 513 (1984); M. Sano, S. Sato, and Y. Sawada, *ibid.* **76**, 945 (1986); J. P. Eckmann and I. Procaccia, *Phys. Rev. A* **34**, 659 (1986).
 [12] T. C. Halsey, M. H. Jensen, L. P. Kadanoff, I. Procaccia,

- and B. I. Schraiman, *Phys. Rev. A* **33**, 1141 (1986).
- [13] H. Fujisaka and H. Shibata, *Prog. Theor. Phys.* **85**, 187 (1991).
- [14] H. Fujisaka and M. Inoue, *Prog. Theor. Phys.* **78**, 268 (1987).
- [15] N. Mori, T. Kobayashi, H. Hata, T. Morita, T. Horita, and H. Mori, *Prog. Theor. Phys.* **81**, 60 (1989).
- [16] H. Fujisaka and M. Inoue, *Phys. Rev. A* **41**, 5302 (1990).
- [17] C. Grebogi, E. Ott, and J. A. Yorke, *Physica* **7D**, 181 (1983); C. Grebogi, E. Ott, F. Romeiras, and J. A. Yorke, *Phys. Rev. A* **36**, 5365 (1987).
- [18] A. Yamaguchi, H. Fujisaka, and M. Inoue, *Phys. Lett. A* **135**, 320 (1989).
- [19] W. H. Steeb, W. Erig, and A. Kunick, *Phys. Lett. A* **93**, 267 (1983).
- [20] J. B. McLaughlin, *J. Stat. Phys.* **24**, 375 (1981); R. W. Leven and B. P. Koch, *Phys. Lett. A* **86**, 71 (1981).
- [21] M. Inoue, T. Kawaguchi, and H. Fujisaka, *Jpn. J. App. Phys. Suppl. No. 2*, 187 (1985).
- [22] W. Just and H. Fujisaka, *Phys. Lett. A* **158**, 385 (1991) and unpublished.